CEAS EuroGNC 2019
"Conference on Guidance, Navigation and Control"
3-5 April 2019 @ Politecnico di Milano, Milan, Italy.

CEAS-GNC-2019-061

Relative orbit-attitude tracking for spacecraft using adaptive fast terminal sliding mode control

Jianqiao Zhang, James D. Biggs, and Zhaowei Sun

Abstract The relative position tracking and attitude synchronization control problem during the process of spacecraft tracking maneuver is addressed in this paper. A robust adaptive sliding mode controller developed on the Special Euclidean Group SE(3) is proposed to guarantee that the spacecraft tracks a prescribed trajectory in the presence of model uncertainties and external disturbances. The mass and inertia of the spacecraft are estimated and the controller adapts to the measurements, so that it is applicable without exact prior knowledge of the model parameters. The closed-loop system is proved to be almost globally asymptotically stable by employing Lyapunov's stability theorem. Finally, simulations for a given scenario are performed to show the performance of the controller.

1 Introduction

Recent years have witnessed significant developments of various space missions, such as spacecraft rendezvous and docking, capture of space targets, spacecraft formation flying, spacecraft hovering, and on-orbit spacecraft maintenance [1, 2, 3, 4]. One of the key technologies for these missions is that the spacecraft has the ability to perform attitude and translational maneuvers simultaneously to track its desired

Jianqiao Zhang
Research Center of Satellite Technology, Harbin Institute of Technology, Harbin, China. Currently, he is a visiting Ph.D. student in the Department of Aerospace Science and Technology, Politecnico di Milano, sponsored by China Scholarship Council. e-mail: zhangjianqiao@hit.edu.cn

James D. Biggs (corresponding author)
Department of Aerospace Science and Technology, Politecnico di Milano, Milan, Italy. e-mail: jamesdouglas.biggs@polimi.it

Zhaowei Sun
Research Center of Satellite Technology, Harbin Institute of Technology, Harbin, China. e-mail: sunzhaowei@hit.edu.cn

trajectory with high accuracy. Traditionally, the modeling and control of orbit and attitude motions are treated separately without considering their coupling, however, for efficient and precise tracking the coupling must be taken into account. In particular, an integrated control based on the relative six-degree-of-freedom (6-DOF) dynamics developed in a unified framework yields better performance than a decoupled design in terms of accuracy and efficiency [5].

To apply this method, two problems need to be solved: (i) Describe the relative dynamics in a framework considering both the relative translational and rotational motions and their coupling; (ii) Develop a control law for this highly nonlinear and high-dimensional structure-preserving (the trajectory is constrained to evolve on SE(3)) system of coupled differential equations. Many coupled relative orbit-attitude models have been developed such as the dual-quaternion representation used in [6, 7, 8], and the exponential coordinates on the Lie group SE(3) used in [3, 4, 5]. However, dual-quaternion in [6, 7, 8] inherits the ambiguities intrinsic of quaternions, and if this property is treated inappropriately, it can cause unwinding problem. In contrast, the matrix form of the Lie group SE(3) is the set of positions and orientations of a rigid spacecraft in three-dimensional Euclidean space, which can represent the spacecraft's motion in a unique and singularity-free way [9].

The 6-DOF dynamics of a spacecraft in orbit around a celestial body is highly nonlinear, and conventional linear control theories fail to perform adequately [10]. Moreover, external disturbance and system uncertainty increase the model complexity and hinder the control accuracy greatly. Therefore, robust nonlinear control techniques is required to control the spacecraft. One example of robust controls, due to their simplicity of implementation, fast response, and effectiveness to deal with uncertainties and nonlinearities, are sliding model controls [11], which have been recognized as an effective tool in 6-DOF spacecraft control in [3, 4, 7, 8, 12]. Adaptive linear sliding mode controller (LSMC) was proposed in [8] to guarantee the asymptotic stability of the closed-loop system. However, the tracking errors only converge fast when they are far away from the origin, and the convergence will be slow when they are close to the origin, leading to a long-term period of inaccuracy. Terminal SMC (TSMC) was used in [4, 7] to address the 6-DOF spacecraft tracking control problem, which can provide a fast local convergence only when the tracking errors are close to the origin. Thus, recently, fast terminal SMC (FTSMC) has been used in [3, 12], for it maintains fast convergence globally. Additionally, these results are obtained on the assumption that the exact information of the inertia and mass of the spacecraft is known in the designed controllers. In contrast, an adaptive FTSMC was proposed in [13] to address 6-DOF spacecraft formation control problem, in which an adaptive term was used to estimate the system parameters.

The purpose of this paper is to investigate the 6-DOF spacecraft tracking control problem based on the relative dynamics developed using exponential coordinates to define a suitable metric to derive the error dynamics on the Lie group SE(3). The model incorporates the structured and unstructured uncertainties, and the orbit-attitude coupling of the spacecraft, as such providing a more realistic model than [5]. Based on the derived model, the main result of this paper is obtained via the adaptive sliding mode technique. By designing an adaptive FTSMC, the almost global

asymptotic stability of the closed-loop system can be guaranteed in the presence of disturbances and without exact knowledge of the system parameters, such as spacecraft mass and inertia which vary over the mission life-time due to fuel usage.

The paper is arranged as follows. The next section gives the problem formulation, including the mathematical model of a rigid spacecraft, the relative dynamics of the spacecraft tracking system, and the control objective. Section 3 presents the adaptive sliding mode controller and the theoretical stability analysis of the closed-loop system. In Section 4, numerical simulations are conducted to illustrate the controller's effectiveness. Finally, Section 5 concludes this paper.

2 Problem Formulation

This section presents the relative dynamics of the spacecraft tracking system and some concepts, which will be used to obtain the main results of this paper.

2.1 Mathematical model of a rigid spacecraft

To develop the dynamic model of a rigid spacecraft, two coordinate frames are defined: a) the standard Earth centered inertial (ECI) frame $\mathscr{F}_I$; b) body-fixed frame $\mathscr{F}_b$, where the origin is located at the mass center of the spacecraft, and its axes coincide with the principal axes of inertia and satisfy the right-hand rule. If $\boldsymbol{R} \in \mathbb{R}^3$ is the position vector of the spacecraft in $\mathscr{F}_I$, and $\boldsymbol{C} \in \mathrm{SO}(3)$ is the coordinate-transformation matrix of the spacecraft from $\mathscr{F}_b$ to $\mathscr{F}_I$, we can obtain the kinematic equations of the spacecraft:

$$\dot{\boldsymbol{R}} = \boldsymbol{C}\boldsymbol{v}, \;\; \dot{\boldsymbol{C}} = \boldsymbol{C}(\boldsymbol{\omega})^{\times} \tag{1}$$

where $\mathrm{SO}(3) = \{\boldsymbol{C} \in \mathbb{R}^{3\times 3} : \boldsymbol{C}^{\mathrm{T}}\boldsymbol{C} = \mathbf{I}_3, \det(\boldsymbol{C}) = 1\}$ is a Lie group, $\mathbf{I}_n$ denotes a $n \times n$ identity matrix, $(\cdot)^{\times}$ represents the skew-symmetric matrix of a vector, and $\boldsymbol{v}$, $\boldsymbol{\omega}$ are the translational velocity and angular velocity expressed in $\mathscr{F}_b$, respectively.

The special Euclidean group SE(3) is also a Lie group, and can be expressed by the semidirect product $\mathrm{SE}(3) = \mathbb{R}^3 \ltimes \mathrm{SO}(3)$, which means that it is a set of all translational and rotational motions of a rigid body [4]. Then the spacecraft configuration can be interpreted using an element $\boldsymbol{\chi}$ of SE(3)

$$\boldsymbol{\chi} = \begin{bmatrix} \boldsymbol{C} & \boldsymbol{R} \\ \mathbf{0}_{1\times 3} & 1 \end{bmatrix} \in \mathrm{SE}(3) \tag{2}$$

and (1) can be changed to [3]

$$\dot{\boldsymbol{\chi}} = \boldsymbol{\chi}(\boldsymbol{V})^{\vee} \tag{3}$$

where $\mathbf{0}_{m\times n}$ is a $m \times n$ zero matrix, $\boldsymbol{V} = \begin{bmatrix} \boldsymbol{\omega}^{\mathrm{T}} & \boldsymbol{v}^{\mathrm{T}} \end{bmatrix}^{\mathrm{T}}$, and $(\cdot)^{\vee} : \mathbb{R}^6 \to \mathfrak{se}(3)$ is

$$\boldsymbol{V}^{\vee} = \begin{bmatrix} \boldsymbol{\omega}^{\times} & \boldsymbol{v} \\ \mathbf{0}_{1\times 3} & 0 \end{bmatrix} \in \mathfrak{se}(3) \tag{4}$$

where $\mathfrak{se}(3)$ is the Lie algebra of SE(3).

The 6-DOF dynamics of the spacecraft expressed in $\mathscr{F}_b$ as given in [3] can be described as:

$$\begin{cases} \boldsymbol{J}\dot{\boldsymbol{\omega}} + \boldsymbol{\omega}^{\times}\boldsymbol{J}\boldsymbol{\omega} = \boldsymbol{M}_{\mathrm{g}} + \boldsymbol{\tau}_{\mathrm{c}} + \boldsymbol{\tau}_{\mathrm{d}} \\ m\dot{\boldsymbol{v}} + m\boldsymbol{\omega}^{\times}\boldsymbol{v} = \boldsymbol{f}_{\mathrm{g}} + \boldsymbol{\psi}_{\mathrm{c}} + \boldsymbol{\psi}_{\mathrm{d}} \end{cases} \tag{5}$$

where $\boldsymbol{J}$ and m are the inertia matrix and mass of the spacecraft, $\boldsymbol{\tau}_{\mathrm{c}}$ and $\boldsymbol{\psi}_{\mathrm{c}}$ are the control torque and force, $\boldsymbol{\tau}_{\mathrm{d}}$ and $\boldsymbol{\psi}_{\mathrm{d}}$ are the external disturbance torque and force, $\boldsymbol{M}_{\mathrm{g}}$ and $\boldsymbol{f}_{\mathrm{g}}$ are the gravity torque and force, respectively. It should be noted that the coupling between the translational motion and the rotational motion is considered in this model. Considering the effects due to the Earth oblateness (J2), the expression of $\boldsymbol{f}_{\mathrm{g}}$ is [6]

$$\boldsymbol{f}_{\mathrm{g}} = -\frac{m\mu\boldsymbol{R}_{\mathrm{b}}}{\|\boldsymbol{R}\|^3} - \frac{3mJ_2\mu R_e^2\boldsymbol{C}^{\mathrm{T}}}{2\|\boldsymbol{R}\|^5}\left(\boldsymbol{D} - \frac{5R_z^2}{\|\boldsymbol{R}\|^2}\boldsymbol{I}_3\right)\boldsymbol{R} \tag{6}$$

$\boldsymbol{M}_{\mathrm{g}}$ is expressed as

$$\boldsymbol{M}_{\mathrm{g}} = 3\left(\frac{\mu}{\|\boldsymbol{R}\|^5}\right)(\boldsymbol{R}_{\mathrm{b}}^{\times}\boldsymbol{J}\boldsymbol{R}_{\mathrm{b}}) \tag{7}$$

where $\mu = 398600.47\mathrm{km}^3/\mathrm{s}^2$ is the gravitational parameter of the Earth, $J_2 = 1.08263 \times 10^{-3}$, $R_e = 6378.14\mathrm{km}$ is the Earth's equatorial radius, $\boldsymbol{R}_b = \boldsymbol{C}^{\mathrm{T}}\boldsymbol{R}$, $\boldsymbol{D} = \mathrm{diag}(1,1,3)$, and R_z is the z-axis component of $\boldsymbol{R}$.

In [14], the inner product of two elements $(\boldsymbol{\omega},\boldsymbol{v}),(\boldsymbol{\eta},\boldsymbol{\psi}) \in \mathfrak{se}(3)$ is defined as a left-invariant metric on SE(3) and expressed as $\ll (\boldsymbol{\omega},\boldsymbol{v}),(\boldsymbol{\eta},\boldsymbol{\psi}) \gg_{\mathfrak{se}(3)} = \boldsymbol{J}\boldsymbol{\omega}\cdot\boldsymbol{\eta} + m\boldsymbol{v}\cdot\boldsymbol{\psi}$. The Lie bracket on $\mathfrak{se}(3)$ is expressed as $[(\boldsymbol{\omega},\boldsymbol{v}),(\boldsymbol{\eta},\boldsymbol{\psi})]_{\mathfrak{se}(3)} = ad_{(\boldsymbol{\omega},\boldsymbol{v})}(\boldsymbol{\eta},\boldsymbol{\psi}) = (\boldsymbol{S}(\boldsymbol{\omega})\boldsymbol{\eta}, \boldsymbol{S}(\boldsymbol{\omega})\boldsymbol{\psi} - \boldsymbol{S}(\boldsymbol{\eta})\boldsymbol{v})$. The operator ad stands for the linear adjoint representation between $\mathfrak{se}(3)$ and SE(3), and its co-adjoint operator ad^* is described on the dual of the Lie algebra and can be described in a matrix form

$$\mathrm{ad}_{\boldsymbol{V}}^{*} = \begin{bmatrix} -\boldsymbol{S}(\boldsymbol{\omega}) & -\boldsymbol{S}(\boldsymbol{v}) \\ \mathbf{0}_{3\times 3} & -\boldsymbol{S}(\boldsymbol{\omega}) \end{bmatrix} \tag{8}$$

Then (5) can be modified as

$$\boldsymbol{\Xi}\dot{\boldsymbol{V}} = \mathrm{ad}_{\boldsymbol{V}}^{*}\boldsymbol{\Xi}\boldsymbol{V} + \boldsymbol{f}(\boldsymbol{\Xi}) + \boldsymbol{\Gamma}_{\mathrm{c}} + \boldsymbol{\Gamma}_{\mathrm{d}} \tag{9}$$

where $\boldsymbol{\Xi} = \mathrm{diag}(\boldsymbol{J}, m\boldsymbol{I})$, $\boldsymbol{f}(\boldsymbol{\Xi}) = \left[\boldsymbol{M}_g^{\mathrm{T}}, \boldsymbol{f}_g^{\mathrm{T}}\right]^{\mathrm{T}}$, $\boldsymbol{\Gamma}_c = \left[\boldsymbol{\tau}_c^{\mathrm{T}}, \boldsymbol{\psi}_c^{\mathrm{T}}\right]^{\mathrm{T}}$, $\boldsymbol{\Gamma}_{\mathrm{d}} = \left[\boldsymbol{\tau}_d^{\mathrm{T}}, \boldsymbol{\psi}_d^{\mathrm{T}}\right]^{\mathrm{T}}$. Thus the mathematical model of a rigid spacecraft can be described by (3) and (9) in a compact form.

2.2 Relative 6-DOF dynamics of the spacecraft tracking system

Let $\boldsymbol{\chi}_d$ and $\boldsymbol{\chi}_a$ be the desired configuration and the actual configuration of the spacecraft respectively, and then we can obtain the configuration tracking error: $\boldsymbol{\chi}_e = (\boldsymbol{\chi}_d)^{-1}\boldsymbol{\chi}_a = \begin{bmatrix} \boldsymbol{C}_e & \boldsymbol{R}_e \\ \boldsymbol{0}_{1\times 3} & 1 \end{bmatrix}$. Using the exponential coordinates on the Lie group SE(3) to express the tracking error, we have

$$\boldsymbol{\eta} = \begin{bmatrix} \boldsymbol{\Phi} \\ \boldsymbol{\varphi} \end{bmatrix} \in \mathbb{R}^6, \text{ and } \boldsymbol{\eta}^{\vee} = \log_{\mathrm{SE(3)}}\boldsymbol{\chi}_{\mathrm{e}} \tag{10}$$

where $\log_{\mathrm{SE(3)}}(\cdot)$ is the logarithm map, which can be calculated as follows [15, 16]

$$\log_{\mathrm{SE(3)}}\boldsymbol{\chi}_1 = \begin{bmatrix} \boldsymbol{\Phi}^{\times} & \boldsymbol{\varphi} \\ \boldsymbol{0}_{1\times 3} & 0 \end{bmatrix} \tag{11}$$

where $\boldsymbol{\Phi}$ and $\boldsymbol{\varphi}$ are the tracking errors described by the exponential coordinates corresponding to attitude and position, respectively.

$$\boldsymbol{\Phi}^{\times} = \begin{cases} \boldsymbol{0} & \theta = 0 \\ \dfrac{\theta}{2\sin\theta}(\boldsymbol{C}_e - \boldsymbol{C}_e^{\mathrm{T}}) & \theta \in (-\pi,\pi), \theta \neq 0 \end{cases} \tag{12}$$

$$\begin{cases} \boldsymbol{\varphi} = \boldsymbol{S}^{-1}(\boldsymbol{\Phi})\boldsymbol{R}_e \\ \boldsymbol{S}(\boldsymbol{\Phi}) = \boldsymbol{I}_3 + \dfrac{1-\cos\theta}{\theta^2}\boldsymbol{\Phi}^{\times} + \dfrac{\theta-\sin\theta}{\theta^3}(\boldsymbol{\Phi}^{\times})^2 \end{cases} \tag{13}$$

where $\theta = \|\boldsymbol{\Phi}\| = \arccos(0.5(\mathrm{tr}(\boldsymbol{C}_e) - 1))$ is the principal rotation angle.

The velocity tracking error expressed in $\mathscr{F}_b$ is

$$\widetilde{\boldsymbol{V}} = \boldsymbol{V} - \mathrm{Ad}_{\boldsymbol{\chi}_e^{-1}}\boldsymbol{V}_d \tag{14}$$

where $\boldsymbol{V}_d$ is the desired velocity and $\mathrm{Ad}_{\boldsymbol{\chi}} = \begin{bmatrix} \boldsymbol{C} & \boldsymbol{0}_{3\times 3} \\ \boldsymbol{R}^{\times}\boldsymbol{C} & \boldsymbol{C} \end{bmatrix}$. Then the kinematics is [4]

$$\dot{\boldsymbol{\eta}} = \boldsymbol{G}(\boldsymbol{\eta})\widetilde{\boldsymbol{V}} \tag{15}$$

The eigenvalues of $\boldsymbol{G}(\boldsymbol{\eta})$ are all positive [3], with expression

$$\boldsymbol{G}(\boldsymbol{\eta}) = \begin{bmatrix} \boldsymbol{A}(\boldsymbol{\Phi}) & \boldsymbol{0} \\ \boldsymbol{T}(\boldsymbol{\Phi},\boldsymbol{\varphi}) & \boldsymbol{A}(\boldsymbol{\Phi}) \end{bmatrix} \tag{16a}$$

$$\boldsymbol{A}(\boldsymbol{\Phi}) = \boldsymbol{I} + \frac{1}{2}(\boldsymbol{\Phi})^{\times} + (\frac{1}{\theta^2} - \frac{1+\cos\theta}{2\theta\sin\theta})(\boldsymbol{\Phi}^{\times})^2 \tag{16b}$$

$$\begin{aligned}\boldsymbol{T}(\boldsymbol{\Phi},\boldsymbol{\varphi}) = &\frac{1}{2}\Big(\boldsymbol{S}(\boldsymbol{\Phi})\boldsymbol{\varphi}\Big)^{\times}\boldsymbol{A}(\boldsymbol{\Phi}) + \Big(\frac{1}{\theta^2} - \frac{1+\cos\theta}{2\theta\sin\theta}\Big)\Big(\boldsymbol{\Phi}\boldsymbol{\varphi}^{\mathrm{T}} + \boldsymbol{\Phi}^{\mathrm{T}}\boldsymbol{\varphi}\boldsymbol{A}(\boldsymbol{\Phi})\Big)\\ &- \frac{\big(1+\cos\theta\big)\big(\theta-\sin\theta\big)}{2\theta\sin^2\theta}\boldsymbol{S}(\boldsymbol{\Phi})\boldsymbol{\varphi}\boldsymbol{\Phi}^{\mathrm{T}}\\ &+ \Big(\frac{\big(1+\cos\theta\big)\big(\theta+\sin\theta\big)}{2\theta^3\sin^2\theta} - \frac{2}{\theta^4}\Big)\boldsymbol{\Phi}^{\mathrm{T}}\boldsymbol{\varphi}\boldsymbol{\Phi}\boldsymbol{\Phi}^{\mathrm{T}}\end{aligned} \tag{16c}$$

Taking the derivative of $\widetilde{\boldsymbol{V}}$ with respect to time and using $\mathrm{d}(\mathrm{Ad}_{\boldsymbol{\chi}_e^{-1}})/\mathrm{dt} = -\mathrm{ad}_{\widetilde{\boldsymbol{V}}}\mathrm{Ad}_{\boldsymbol{\chi}_e^{-1}}$ proved in [4], the acceleration of the spacecraft is

$$\dot{\widetilde{\boldsymbol{V}}} = \dot{\boldsymbol{V}} + \mathrm{ad}_{\widetilde{\boldsymbol{V}}}\mathrm{Ad}_{\boldsymbol{\chi}_e}^{-1}\boldsymbol{V}_d - \mathrm{Ad}_{\boldsymbol{\chi}_e}^{-1}\dot{\boldsymbol{V}}_d \tag{17}$$

Taking (9) into (17), one can obtain

$$\boldsymbol{\Xi}\dot{\widetilde{\boldsymbol{V}}} = \mathrm{ad}_{\boldsymbol{V}}^{*}\boldsymbol{\Xi}\boldsymbol{V} + \boldsymbol{f}(\boldsymbol{\Xi}) + \boldsymbol{\Gamma}_{\mathrm{c}} + \boldsymbol{\Gamma}_{\mathrm{d}} + \boldsymbol{\Xi}(\mathrm{ad}_{\widetilde{\boldsymbol{V}}}\mathrm{Ad}_{\boldsymbol{\chi}_e}^{-1}\boldsymbol{V}_d - \mathrm{Ad}_{\boldsymbol{\chi}_e}^{-1}\dot{\boldsymbol{V}}_d) \tag{18}$$

For actual system, model uncertainties can not be ignored. Thus, we use $\boldsymbol{\Xi}_1 = \boldsymbol{\Xi} + \Delta\boldsymbol{\Xi}$ to express the total moment of the inertia matrix and the mass of the spacecraft, where $\Delta\boldsymbol{\Xi}$ is the uncertainty part. $\boldsymbol{\Xi}_1^{-1} = \boldsymbol{\Xi}^{-1} + \Delta\widetilde{\boldsymbol{\Xi}}$, where $\Delta\widetilde{\boldsymbol{\Xi}}$ is also the uncertainty part. Thus the relative 6-DOF dynamics of the tracking system can be rewritten as:

$$\boldsymbol{\Xi}\dot{\widetilde{\boldsymbol{V}}} = \mathrm{ad}_{\boldsymbol{V}}^{*}\boldsymbol{\Xi}\boldsymbol{V} + \boldsymbol{\Xi}(\mathrm{ad}_{\widetilde{\boldsymbol{V}}}\mathrm{Ad}_{\boldsymbol{\chi}_e}^{-1}\boldsymbol{V}_d - \mathrm{Ad}_{\boldsymbol{\chi}_e}^{-1}\dot{\boldsymbol{V}}_d) + \Delta\boldsymbol{\Gamma}_d + \boldsymbol{\Gamma}_c + \boldsymbol{f}(\boldsymbol{\Xi}) \tag{19}$$

where $\Delta\boldsymbol{\Gamma}_d = \boldsymbol{\Xi}\Delta\widetilde{\boldsymbol{d}}$, $\Delta\widetilde{\boldsymbol{d}} = \Delta\widetilde{\boldsymbol{\Xi}}\big(\mathrm{ad}_{\boldsymbol{V}}^{*}\boldsymbol{\Xi}_1\boldsymbol{V} + \boldsymbol{\Gamma}_c + \boldsymbol{f}(\boldsymbol{\Xi})\big) + \boldsymbol{\Xi}^{-1}\mathrm{ad}_{\boldsymbol{V}}^{*}\Delta\boldsymbol{\Xi}\boldsymbol{V} + \boldsymbol{\Xi}_1^{-1}\big(\boldsymbol{\Gamma}_d + \boldsymbol{f}(\boldsymbol{\Xi}_1) - \boldsymbol{f}(\boldsymbol{\Xi})\big)$ and $\Delta\boldsymbol{\Gamma}_d$ is the lumped disturbance of the system and satisfies the following assumption.

Assumption 1 *The total disturbance of the spacecraft $\Delta\boldsymbol{\Gamma}_d$ is assumed to be bounded, which satisfies*

$$|\Delta\boldsymbol{\Gamma}_{di}| \leqslant \delta_i, i = 1,2,\ldots,6 \tag{20}$$

where $\boldsymbol{\delta} \in \mathbb{R}^{6\times 1}$ is a positive constant vector.

Lemma 1. *[3] $V(t)$ is a continuous positive definite function. If the following differential inequality holds*

$$\dot{V}(t) + \varpi_1 V(t) + \varpi_2 V^{\varpi}(t) \leq 0, \forall t > t_0 \tag{21}$$

where $\varpi_1 > 0, \varpi_2 > 0$, and $0 < \varpi < 1$, then $V(t)$ can reach the equilibrium in finite time t_f, where

$$t_f \leq t_0 + \frac{1}{\varpi_1(1-\varpi)}\ln\frac{\varpi_1 V^{1-\varpi}(t_0) + \varpi_2}{\varpi_2} \tag{22}$$

Control objective: The purpose of this paper is to design a control scheme $\boldsymbol{\Gamma}_c$, such that the trajectory of the spacecraft can track its desired states in the presence of model uncertainties and external disturbances, and the resulting closed-loop system should be asymptotically stable. Here, the desired trajectory is computed offline based on (9) in an ideal environment (without control torques and forces, system uncertainties, and external disturbances).

3 Adaptive sliding mode controller design

First, we define the FTSM in the form of

$$\boldsymbol{S} = \widetilde{\boldsymbol{V}} + \boldsymbol{\vartheta}_1 \boldsymbol{\eta} + \boldsymbol{\vartheta}_2 sig^{\alpha}(\boldsymbol{\eta}) \tag{23}$$

where $\boldsymbol{\vartheta}_1, \boldsymbol{\vartheta}_2 \in \mathbb{R}^{6\times 6}$ are positive definite diagonal matrices, and $\alpha \in (0.5, 1)$ to avoid sliding surface singularity, $\mathrm{sig}^{\alpha}(\boldsymbol{x}) = \left[\, |x_1|^{\alpha}\mathrm{sgn}(x_1), \cdots, |x_6|^{\alpha}\mathrm{sgn}(x_6) \,\right]^{\mathrm{T}}$, sgn is the sign function.

Denoting $\boldsymbol{f}(\boldsymbol{\eta}) = \boldsymbol{\vartheta}_1 \dot{\boldsymbol{\eta}} + \alpha \boldsymbol{\vartheta}_2 \mathrm{diag}(|\boldsymbol{\eta}|^{\alpha-1})\dot{\boldsymbol{\eta}}$ and $\boldsymbol{f}(\boldsymbol{V}_d) = \mathrm{ad}_{\widetilde{\boldsymbol{V}}}\mathrm{Ad}^{-1}_{\boldsymbol{\chi}_e}\boldsymbol{V}_d - \mathrm{Ad}^{-1}_{\boldsymbol{\chi}_e}\dot{\boldsymbol{V}}_d$, then we have

$$\boldsymbol{\Xi}\dot{\boldsymbol{S}} = \mathrm{ad}^{*}_{\boldsymbol{V}}\boldsymbol{\Xi}\boldsymbol{V} + \boldsymbol{\Xi}\big(\boldsymbol{f}(\boldsymbol{\eta}) + \boldsymbol{f}(\boldsymbol{V}_d)\big) + \Delta\boldsymbol{\Gamma}_d + \boldsymbol{\Gamma}_c + \boldsymbol{f}(\boldsymbol{\Xi}) \tag{24}$$

To estimate the inertia and the mass of the spacecraft, motivated by [6], for a vector $\boldsymbol{x} = [x_1, x_2, x_3]^{\mathrm{T}} \in \mathbb{R}^3$, we define a linear operator $\boldsymbol{H}$ as follows

$$\boldsymbol{H}(\boldsymbol{x}) = \begin{bmatrix} x_1 & 0 & 0 & 0 & x_3 & x_2 \\ 0 & x_2 & 0 & x_3 & 0 & x_1 \\ 0 & 0 & x_3 & x_2 & x_1 & 0 \end{bmatrix} \tag{25}$$

Then we can obtain $\boldsymbol{J}\boldsymbol{x} = \boldsymbol{H}(\boldsymbol{x})\boldsymbol{\nu}(\boldsymbol{J})$, $\boldsymbol{\nu}(\boldsymbol{J}) = [\boldsymbol{J}_{11}, \boldsymbol{J}_{22}, \boldsymbol{J}_{33}, \boldsymbol{J}_{23}, \boldsymbol{J}_{13}, \boldsymbol{J}_{12}]^{\mathrm{T}} \in \mathbb{R}^6$. Thus $\boldsymbol{\Xi}\dot{\boldsymbol{S}}$ can be expressed as

$$\boldsymbol{\Xi}\dot{\boldsymbol{S}} = \boldsymbol{Y}\boldsymbol{\nu}(\boldsymbol{\Xi}) + + \Delta\boldsymbol{\Gamma}_d + \boldsymbol{\Gamma}_c \tag{26}$$

where $\boldsymbol{\nu}(\boldsymbol{\Xi}) = [(\boldsymbol{J})_{11}, (\boldsymbol{J})_{22}, (\boldsymbol{J})_{33}, (\boldsymbol{J})_{23}, (\boldsymbol{J})_{13}, (\boldsymbol{J})_{12}, m]^{\mathrm{T}}$,
and $\boldsymbol{Y} = \mathrm{diag}\big(\boldsymbol{Y}_{\mathrm{attitude}}, \boldsymbol{Y}_{\mathrm{orbit}}\big) \in \mathbb{R}^{6\times 7}$. The expressions of $\boldsymbol{Y}_{\mathrm{attitude}} \in \mathbb{R}^{3\times 6}$ and $\boldsymbol{Y}_{\mathrm{orbit}} \in \mathbb{R}^{3\times 1}$ are: $\boldsymbol{Y}_{\mathrm{attitude}} = \boldsymbol{H}([\boldsymbol{f}(\boldsymbol{\eta}) + \boldsymbol{f}(\boldsymbol{V}_d)]_1) - \boldsymbol{\omega}^{\times}\boldsymbol{H}(\boldsymbol{\omega}) + 3\dfrac{\mu}{\|\boldsymbol{R}\|^5}\boldsymbol{R}_{\mathrm{b}}^{\times}\boldsymbol{H}(\boldsymbol{R}_{\mathrm{b}})$,
and $\boldsymbol{Y}_{\mathrm{orbit}} = [\boldsymbol{f}(\boldsymbol{\eta}) + \boldsymbol{f}(\boldsymbol{V}_d)]_2 - \dfrac{\mu\boldsymbol{R}_{\mathrm{b}}}{\|\boldsymbol{R}\|^3} - \dfrac{3J_2\mu R_e^2\boldsymbol{C}^{\mathrm{T}}}{2\|\boldsymbol{R}\|^5}\big(\boldsymbol{D} - \dfrac{5R_z^2}{\|\boldsymbol{R}\|^2}\boldsymbol{I}_3\big)\boldsymbol{R} - \boldsymbol{\omega}^{\times}\boldsymbol{v}$, where
$[\boldsymbol{f}(\boldsymbol{\eta}) + \boldsymbol{f}(\boldsymbol{V}_d)]_1 = [\boldsymbol{f}_1(\boldsymbol{\eta}) + \boldsymbol{f}_1(\boldsymbol{V}_d), \boldsymbol{f}_2(\boldsymbol{\eta}) + \boldsymbol{f}_2(\boldsymbol{V}_d), \boldsymbol{f}_3(\boldsymbol{\eta}) + \boldsymbol{f}_3(\boldsymbol{V}_d)]^{\mathrm{T}}$ and
$[\boldsymbol{f}(\boldsymbol{\eta}) + \boldsymbol{f}(\boldsymbol{V}_d)]_2 = [\boldsymbol{f}_4(\boldsymbol{\eta}) + \boldsymbol{f}_4(\boldsymbol{V}_d), \boldsymbol{f}_5(\boldsymbol{\eta}) + \boldsymbol{f}_5(\boldsymbol{V}_d), \boldsymbol{f}_6(\boldsymbol{\eta}) + \boldsymbol{f}_6(\boldsymbol{V}_d)]^{\mathrm{T}}$. To this end, Theorem 1 is proposed to realize the spacecraft trajectory tracking control.

Theorem 1. *For the spacecraft tracking system governed by (15) and (19), if **Assumption 1** is satisfied and the controller is designed as*

$$\boldsymbol{\Gamma}_c = -\boldsymbol{Y}\hat{\boldsymbol{\nu}}(\boldsymbol{\Xi}) - \boldsymbol{K}_1\boldsymbol{S} - \boldsymbol{K}_2\mathrm{sgn}(\boldsymbol{S}) \tag{27}$$

where $\boldsymbol{K}_1 = \mathrm{diag}(k_{11},\cdots,k_{16}) > 0$, $\boldsymbol{K}_2 = \mathrm{diag}(k_{21},\cdots,k_{26}) > 0$ and $\hat{\boldsymbol{\nu}}(\boldsymbol{\Xi})$ is the estimation of $\boldsymbol{\nu}(\boldsymbol{\Xi})$. The updated law of $\hat{\boldsymbol{\nu}}(\boldsymbol{\Xi})$ is

$$\dot{\hat{\boldsymbol{\nu}}}(\boldsymbol{\Xi}) = \boldsymbol{\Lambda}\boldsymbol{Y}^{\mathrm{T}}\boldsymbol{S} \tag{28}$$

where $\boldsymbol{\Lambda} \in \mathbb{R}^{7\times 7}$ is a positive definite diagonal matrix. If $k_{2i} > \delta_i, i = 1,2,\ldots,6$ is satisfied, then the closed-loop system is almost globally asymptotically stable.

Proof. Let a Lyapunov function candidate with the form of

$$V_1 = \frac{1}{2}\boldsymbol{S}^{\mathrm{T}}\boldsymbol{\Xi}\boldsymbol{S} + \frac{1}{2}\tilde{\boldsymbol{\nu}}^{\mathrm{T}}(\boldsymbol{\Xi})\boldsymbol{\Lambda}^{-1}\tilde{\boldsymbol{\nu}}(\boldsymbol{\Xi}) \tag{29}$$

where $\tilde{\boldsymbol{\nu}}(\boldsymbol{\Xi}) = \hat{\boldsymbol{\nu}}(\boldsymbol{\Xi}) - \boldsymbol{\nu}(\boldsymbol{\Xi})$. Calculating the first order derivative of V_1 with respect to time and substituting (26), (27), and (28) into it, we can obtain

$$\begin{aligned}
\dot{V}_1 &= \boldsymbol{S}^{\mathrm{T}}\boldsymbol{\Xi}\dot{\boldsymbol{S}} + \tilde{\boldsymbol{\nu}}^{\mathrm{T}}(\boldsymbol{\Xi})\boldsymbol{\Lambda}^{-1}\dot{\tilde{\boldsymbol{\nu}}}(\boldsymbol{\Xi}) = \boldsymbol{S}^{\mathrm{T}}\big(\boldsymbol{Y}\boldsymbol{\nu}(\boldsymbol{\Xi}) + \Delta\boldsymbol{\Gamma}_d + \boldsymbol{\Gamma}_c\big) + \tilde{\boldsymbol{\nu}}^{\mathrm{T}}(\boldsymbol{\Xi})\boldsymbol{Y}^{\mathrm{T}}\boldsymbol{S} \\
&= \boldsymbol{S}^{\mathrm{T}}\big(-\boldsymbol{K}_1\boldsymbol{S} - \boldsymbol{K}_2\mathrm{sgn}(\boldsymbol{S}) + \Delta\boldsymbol{\Gamma}_d\big) \\
&\leq -\boldsymbol{S}^{\mathrm{T}}\boldsymbol{K}_1\boldsymbol{S} - \sum_{i=1}^{6}\big(k_{2i}\,|\boldsymbol{S}_i| - \delta_i\,|\boldsymbol{S}_i|\big) \leq -\rho\,\|\boldsymbol{S}\| \leq 0
\end{aligned} \tag{30}$$

where $\rho = \min(k_{2i} - \delta_i)$. Integrating both sides of (30) from 0 to ∞, yields

$$V_1(0) - V_1(\infty) \geq \rho\int_0^t \|\boldsymbol{S}\|\,dt \tag{31}$$

The term on the left-hand side is bounded, thus $\boldsymbol{S} \in L_1$, and further $\boldsymbol{S} \in L_\infty$. From the spacecraft dynamics, it can be concluded that $\dot{\boldsymbol{S}} \in L_\infty$. Hence, by the Barbalat's lemma in [18], it can be concluded that $\lim_{t\to\infty}\|\boldsymbol{S}\| = 0$, which implies that $\tilde{\boldsymbol{V}} = -\boldsymbol{\vartheta}_1\boldsymbol{\eta} - \boldsymbol{\vartheta}_2 sig^{\alpha}(\boldsymbol{\eta})$. Then we consider another Lyapunov function $V_2 = \frac{1}{2}\boldsymbol{\eta}^{\mathrm{T}}\boldsymbol{\eta}$. Differentiating V_2 with respect to time and taking $\tilde{\boldsymbol{V}}$ into it, we have

$$\dot{V}_2 = \boldsymbol{\eta}^{\mathrm{T}}\dot{\boldsymbol{\eta}} \leq -\bar{\vartheta}_1 V_2 - \bar{\vartheta}_2 V_2^{\frac{1+\alpha}{2}} \tag{32}$$

where $\bar{\vartheta}_1 = 2\lambda_{\min}(\boldsymbol{G}(\boldsymbol{\eta})\boldsymbol{\vartheta}_1) > 0$ and $\bar{\vartheta}_2 = 2^{(1+\alpha)/2}\lambda_{\min}(\boldsymbol{G}(\boldsymbol{\eta})\boldsymbol{\vartheta}_2) > 0$. Thus by using Lemma 1, we can obtain that $\boldsymbol{\eta} = 0, \tilde{\boldsymbol{V}} = 0$ can be reached in finite time after $\boldsymbol{S}$ reaches the origin. Since when $\theta = \pm\pi$, the exponential coordinates for the attitude are not uniquely defined, thus the designed control law can reduce the configuration tracking errors to the origin except those that differ from the desired trajectory in orientation by a π radian rotation. Therefore, we can conclude that the closed-loop

system is almost globally asymptotically stable. Thereby, the proof of Theorem 1 has been completed.

4 Simulation results

To verify the effectiveness of the proposed adaptive sliding mode controller, simulations for a given scenario are presented in this section. The desired trajectory of the spacecraft is assumed to follow a circle orbit with altitude 400 km and inclination 45°, and its body fixed frame is always perfectly aligned with the orbit frame. The nominal parts of the inertia matrix and the mass of the spacecraft are assumed to be: $m = 105\text{kg}$ and $\boldsymbol{J}_1 = \begin{bmatrix} 25 & 1 & 0.5 \\ 1 & 22 & 1.2 \\ 0.5 & 1.2 & 23 \end{bmatrix} \text{kg} \cdot \text{m}^2$. The uncertainty parts of the mass and inertia matrix considering fuel cost are chosen as $\Delta\boldsymbol{\Xi} = \text{diag}(0.12\boldsymbol{J}, 0.03m\boldsymbol{I}_3)$. The disturbances considering magnetic torque, solar radial pressure force, and aerodynamics that the spacecraft suffers are assumed to be [13, 17]: $\boldsymbol{\tau}_d = 10^{-4} \cdot \left[\sin(1+0.12t), \cos(1+0.15t), \sin(1+0.18t)\right]^{\text{T}} \text{N} \cdot \text{m}$, $\boldsymbol{\psi}_d = 10^{-5} \cdot [-1.025,\ 6.248,\ -2.215]^{\text{T}} \sin(2\pi \|\boldsymbol{\omega}_d\| t)$ N.

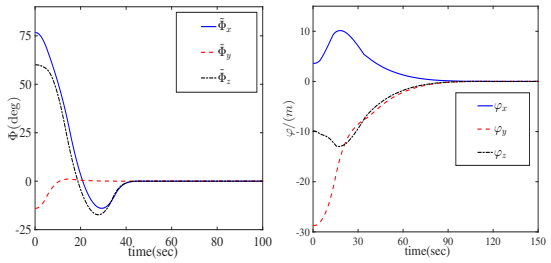

Fig. 1 Time responses of attitude (left) and position (right) tracking errors.

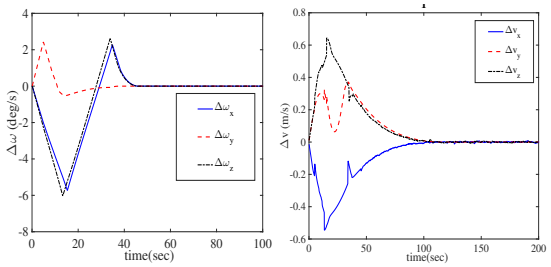

Fig. 2 Time responses of angular velocity (left) and translational velocity (right) tracking errors.

Initially, the trajectory tracking errors are: the relative position error is $\Delta\boldsymbol{R} = [15, -10, -20]^{\text{T}}\text{m}$ in $\mathscr{F}_b$, the transformation matrix is assumed to be different from

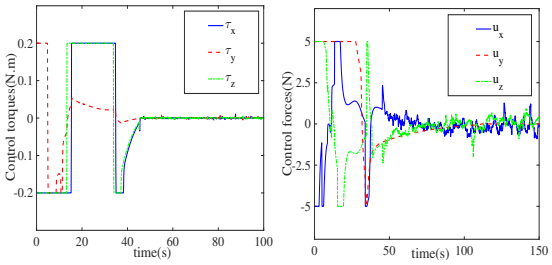

Fig. 3 Time responses of control torques (left) and control forces (right).

the desired one through [3,1,3] with Euler angles $[\pi/4, \pi/4, \pi/4]$, and $\widetilde{\boldsymbol{V}} = 0$. To guarantee the global asymptotical stability of the closed-loop system, the controller parameters are selected as: the related parameters of the sliding mode are $\boldsymbol{\vartheta}_1 = \mathrm{diag}(0.1\boldsymbol{I}_3, 0.02\boldsymbol{I}_3)$, $\boldsymbol{\vartheta}_2 = \mathrm{diag}(0.1\boldsymbol{I}_3, 0.05\boldsymbol{I}_3)$, $\alpha = 2/3$; the parameters in (27) are $\boldsymbol{K}_1 = \mathrm{diag}(5\boldsymbol{I}_6)$, $\boldsymbol{K}_2 = \mathrm{diag}(2\boldsymbol{I}_3, 1.2\boldsymbol{I}_3)$, $\boldsymbol{\Lambda} = \mathrm{diag}(12, 12, 12, 12, 12, 12, 1.5)$, and the initial estimation of $\hat{\boldsymbol{\nu}}(\boldsymbol{\Xi})$ is set as $[25, 25, 25, 0, 0, 0, 100]^{\mathrm{T}}$. Moreover, a continuous function $\boldsymbol{S}/(\|\boldsymbol{S}\| + \varepsilon)$ is employed to approximate $\mathrm{sgn}(\boldsymbol{S})$ to reduce chattering, where ε is a small positive constant. Furthermore, due to physical limitations on actuator, actuator saturation should be considered. Thus, we assume the bounded force and torque that the spacecraft actuators can offer are $\tau_{\mathrm{cmax}} = 0.2\mathrm{N} \cdot \mathrm{m}$ [17] and $\psi_{\mathrm{cmax}} = 5\mathrm{N}$ [13], respectively.

The simulation results are presented in Figs. 1-3. Figure 1 shows the time responses of attitude and position tracking errors in terms of the exponential coordinates with respect to the desired trajectory, and the tracking errors of angular velocity and translational velocity are presented in Figure 2. It can be seen that under the control torques in Figure 3, the rotational motion tracking errors fall to the tolerance within 50s. While, under the control forces in Figure 3, the convergence time of the orbit tracking errors is about 100s. Moreover, from the curves of the control torques and forces acting on the spacecraft, we can see that the outputs of the spacecraft actuators are bounded.

5 Conclusions

A robust adaptive FTSMC has been presented that is able to efficiently and robustly track a 6-DOF rigid spacecraft reference motion in the presence of model uncertainties and external disturbances, which are inherent in spacecraft system such as variations in mass and inertia as well as in uncertain environments such as inhomogeneous gravity fields, solar radiation pressure, magnetic fields and atmospheric density. More specifically, based on the relative 6-DOF model, the sliding surface is constructed, and by choosing the parameters properly, the singularity in traditional sliding mode control can be avoided. The controller is developed to include an adaptive term that guarantees the almost global asymptotic stability of the system without exact knowledge of the inertia and mass of the spacecraft. Finally, simulations are

performed to assess the controller's effectiveness and feasibility, from which we can conclude that the results in this paper can provide a theoretical basis for spacecraft tracking control design in practice.

References

1. Singla, P., Subbarao, K., Junkins, J. L.: Adaptive output feedback control for spacecraft rendezvous and docking under measurement uncertainty. J. Guid. Control Dyn. **29**(4), 892–902 (2006)
2. Gui, H., Ruiter, A. H. J. D.: Control of asteroid-hovering spacecraft with disturbance rejection using position-only measurements. J. Guid. Control Dyn. **40**(10), 2401–2416 (2017)
3. Zhang, J., Ye, D., Sun, Z., Liu, C.: Extended state observer based robust adaptive control on SE(3) for coupled spacecraft tracking maneuver with actuator saturation and misalignment. Acta Astronaut. **143**, 221–233 (2018)
4. Lee, D., Vukovich, G.: Robust adaptive terminal sliding mode control on SE(3) for autonomous spacecraft rendezvous and docking. Nonlinear Dyn. **83**(4), 2263–2279 (2016)
5. Jiang, L., Wang, Y., Xu, S.: Integrated 6-DOF orbit-attitude dynamical modeling and control using geometric mechanics. Int. J. Aerosp. Eng. **2017**, Article ID 4034328 (2017)
6. Gui, H., Vukovich, G.: Dual-quaternion-based adaptive motion tracking of spacecraft with reduced control effort. Nonlinear Dyn. **83**(1-2), 597–614 (2016)
7. Wang, J., Liang, H., Sun, Z., Zhang, S., Liu, M.: Finite-time control for spacecraft formation with dual-number-based description. J. Guid. Control Dyn. **35**(3), 950–962 (2012)
8. Wu, J., Liu, K., Han, D.: Adaptive sliding mode control for six-DOF relative motion of spacecraft with input constraint. Acta Astronaut. **87**, 64–76 (2013)
9. Biggs, J. D., Colley, L.: Geometric attitude motion planning for spacecraft with pointing and actuator constraints. J. Guid. Control Dyn. **39**(7), 1672–1677 (2016)
10. Xin, M., Pan, H.: Integrated nonlinear optimal control of spacecraft in proximity operations. Int. J. Control **83**(2), 347–363 (2010)
11. Xiao, B., Yin, S.: Velocity-free fault-tolerant and uncertainty attenuation control for a class of nonlinear systems. IEEE Trans. Ind. Electron. **63**(7), 4400–4411 (2016)
12. Ye, D., Zhang, J., Sun, Z.: Extended state observerbased finite-time controller design for coupled spacecraft formation with actuator saturation. Adv. Mech. Eng. **9**(4), 168781401769641 (2017)
13. Zhang, J., Ye, D., Biggs, J. D., Sun, Z.: Finite-time relative orbit-attitude tracking control for multi-spacecraft with collision avoidance and changing network topologies. Adv. Space Res. **63**(3), 1161–1175 (2019)
14. Maithripala, D. H. S., Dayawansa, W. P., Berg, J. M.: Intrinsic observer-based stabilization for simple mechanical systems on Lie groups. SIAM J. Control Optim. **44**(5), 1691–1711 (2005)
15. Biggs, J. D., Horri, N.: An exponentially fast attitude tracking controller on the rotation group. In: 65th International Astronautical Congress, 29 September-3 October, 2014, Toronto, Canada, IAC-14-C1.4.3
16. Bullo, F., Murray, R.M.: Proportional derivative (PD) control on the Euclidean group. In: Proceedings of the 3rd European Control Conference, vol. 2, pp. 1091–1097. European Control Association, Zurich, Switzerland (1995)
17. Xiao, B., Hu, Q., Zhang, Y., Huo, X.: Fault-tolerant tracking control of spacecraft with attitude-only measurement under actuator failures. J. Guid. Control Dyn. **37**(3), 838–849 (2014)
18. Slotine J. E., Li W.: Applied nonlinear control. Prentice hall Englewood Cliffs, NJ. **199**(1) (1991)